DEPARTMENT OF INTERNATIONAL AND EUROPEAN ECONOMIC STUDIES

ATHENS UNIVERSITY OF ECONOMICS AND BUSINESS

Regional Climate Change Policy under Positive Feedbacks and Strategic Interactions

William Brock

Anastasios Xepapadeas

Working Paper Series

18-05

February 2018

Regional Climate Change Policy under Positive Feedbacks and Strategic Interactions[1]

William Brock* and Anastasios Xepapadeas**

*Economics Department, University of Wisconsin
and University of Missouri, wbrock@ssc.wisc.edu,

**Department of International and European Economic Studies,
Athens University of Economics and Business,
and Department of Economics, University of Bologna, xepapad@aueb.gr

February 20, 2018

[1]We are grateful to an anonymous reviewer for valuable comments and suggestions on an earlier draft of the paper.

Abstract

The surface albedo feedback, along with heat and moisture transport from the Equator to the Poles, is associated with polar amplification which is a well-established scientific fact. The present paper extends Brock and Xepapadeas (2017a) to a non-cooperative framework with polar amplification, where regions decide emissions by maximizing own welfare. This can be regarded as a case of regional non-cooperation regarding climate change. Open loop and feedback solutions are derived and compared, in terms of temperature paths and welfare, with the cooperative solution. Carbon taxes which could bridge the gap between cooperative and non-cooperative emissions path are also derived. Finally, the framework is extended to a Ramsey set-up in which it is shown how the regional climate model can be coupled with standard optimal growth models. Numerical simulations confirm the theoretical results and provide insights about the size and the direction of deviations between the cooperative and the non-cooperative solutions.

JEL Classification: Q54 Q58

Keywords: Arctic amplification, Spatial heat and moisture transport, Optimal policy, Emission taxes, Open loop, Feedback Nash Equilibrium.

1 Introduction

Understanding climate change along with its economic dimension is a complex issue that involves climate science, economics, and their interactions. The study of climate change economics is further complicated by feedbacks within the climate system. Climate feedbacks are Earth system interactions that are set in motion by the effect of a forcing factor on one part of the system. Feedbacks amplify (positive feedback) or dampen (negative feedback) the effect of a forcing factor, or cause additional change in another part of the system.

One of the well established feedbacks of the climate system is Arctic Amplification (AA). Evidence indicates that the Arctic warms faster because significant positive feedbacks are taking place in the region. According to the IPCC (2013, p. 396):

"Polar amplification[1] occurs if the magnitude of zonally averaged surface temperature change at high latitudes exceeds the globally averaged temperature change, in response to climate forcings and on time scales greater than the annual cycle."

Recent studies provide an indicatation of the magnitude of AA. Bekryaev et al. (2010), using an extensive data set of monthly surface air temperature, document a high-latitude ($>$ 60N) warming rate of 1.36C/century for 1875-2008, with the trend being almost two times stronger than the Northern Hemisphere trend of 0.79C/century.

AA, which represents a feedback with geographical (i.e., spatial) origin, introduces a new aspect into the study of the regional impacts of climate change. This aspect relates to the possibility that temperature change in a location like the Arctic may generate damages to a location farther away, e.g., the South. This is a kind of spatial spillover which adds another dimension to the process that associates regional damages to the global mean temperature or regional temperature, in addition to the specific characteristics of the region such as production characteristics (e.g., agriculture vs services) or local natural characteristics (e.g., proximity to the sea and elevation).

In this context AA could be a major source of damage flows to southern regions as current research suggests.[2]

> "As emissions of greenhouse gases continue unabated, therefore, the continued amplification of Arctic warming should favour

[1] Polar amplification refers to the relatively faster warming of the Poles (North and South). Since, however, the large majority of the scientific evidence and the analysis in the present paper focus on the faster warming of the North Pole, we will refer to the phenomenon as Arctic Amplification throughout the paper.

[2] It should be noted that heat transfer toward the Poles could be beneficial to regions around the Equator, since it reduces temperatures and thus damages in these regions.

an increased occurrence of extreme events caused by prolonged weather conditions." (Francis and Skific, 2015)

"The effects of climate change on extreme weather are a topic of intense scientific interest and of vital societal impact. Some of these effects are clear – such as more severe heat waves, more frequent heavy precipitation events, and more persistent droughts – but other less direct influences are still 'up in the air'." (Francis, 2017)

The two major mechanisms associated with AA are heat transport from the Equator to the Poles and the surface albedo effect. AA, apart from the potential inducement of extreme events, is also associated with another important feedback, the Arctic permafrost. According to the IPCC (2013, p.9): "There is high confidence that permafrost temperatures have increased in most regions since the early 1980s. Observed warming was up to 3°C in parts of northern Alaska (early1980s to mid-2000s) and up to 2°C in parts of the Russian European North (1971 to 2010)." Permafrost thawing and release of greenhouse gases (GHGs) introduces the concept of a "damage reservoir" (Brock et al., 2014a) where a local change in the temperature, the AA in this case, generates global damages.[3]

Under conditions of AA due to heat transport and surface albedo feedbacks, an increase in temperature in the North could generate a "flow" of damages to the South.[4] This can be regarded as similar to an upstream–downstream pollution problem, but the upstream problem is not generated by the actions of the upstream agent but rather by the collective action of agents. On the other hand, if some agents located upstream are large emitters and they realize that some of the damages will take place downstream, they might have less incentive to mitigate their emissions.

However, although AA is regarded by climate science as a near universal feature of climate model simulations of the planet's response to increasing atmospheric GHG concentrations, this feature has been largely ignored by the economics of climate science, despite evidence suggesting that AA could have important economic implications[5] such as loss of Arctic sea ice which in turn has consequences for melting land ice; melting land ice associated with a potential meltdown of Greenland and West Antarctica ice sheets (see Lenton et al., 2008); and thawing of permafrosts.

All the above are positive feedbacks which should be included in economic models. As pointed out by Dietz and Stern (2015), the science of

[3] According to a recent *New York Times* article, rising temperatures in Alaska could result in a complete thaw of its permafrost by 2050 (Fountain, 2017). For the costs of Arctic change, see, for example, Whiteman et al. (2013).

[4] In Narem et al. (2018), table 2 suggests that sea level rise associated with the melting of land ice in Greenland can be associated with AA-induced transport of damages towards the South.

[5] See Brock and Xepapadeas (2017b) for details.

climate change has been running years ahead of the economics of climate change. One way of bringing the economics of climate change closer to climate science in terms of AA is to introduce AA induced by spatial heat transport and surface albedo effects into an economic model of climate change and to explore their impacts on the design of climate policy in the form of emission paths and carbon taxes. This approach can be regarded as extending the literature on the optimal taxation of GHG emissions by accounting for the AA effect.

In a recent paper by Brock and Xepapadeas (2017a), the AA effect was modelled in the context of a two-region model (Alexeev et al. 2005; Langen and Alexeev, 2007; Alexeev and Jackson, 2012) with heat transport from the Equator to the Poles and potential surface albedo effects. Region or box 2 according to the climate science terminology represents the higher latitudes (30°N to 90°N) and region or box 1 the lower latitudes (0° to 30°N). The two-box model was coupled with a simple welfare-maximization problem to derive the optimal GHG emissions path in the two regions. This solution can be regarded as the social planner's solution or the cooperative solution.

The purpose of the present paper is to extend Brock and Xepapadeas (2017a) to a non-cooperative framework with AA, in which regions decide emissions by maximizing own welfare. This can be regarded as the case of regional non-cooperation regarding climate change. Open loop and feedback solutions are derived and compared, in terms of temperature paths and welfare, with the cooperative solution. Carbon taxes which could bridge the gap between cooperative and non-cooperative emissions paths are also derived. Finally the framework is extended to a Ramsey set-up in which it is shown how the regional climate model can be coupled with standard optimal growth models.

2 Modeling Arctic Amplification

2.1 Heat Transport

In climate science terminology, models with a carbon cycle and no spatial dimension are zero-dimensional models. These models do not include spatial effects due to heat transportation across space because heat transport cannot take place across locations, since there are no distinct locations in the model. In contrast, the one- or two-dimensional energy balance climate models (EBCMs) model heat transport across latitudes or across latitudes and longitudes in continuous space (e.g. North, 1975a, 1975b; North et al., 1981; Wu and North, 2007). In these models the incoming absorbed radiant heat at a given latitude, in equilibrium, is not matched by the net outgoing radiation and the difference is made by the meridional divergence of heat flux which is modelled by a diffusion term which explicitly introduces the spatial dimension stemming from the heat transport into the climate model.

EBCMs in continuous time with a spatial diffusion coefficient are quite complex to handle in economic modeling since they require dynamic optimization with partial differential equations as constraints (see Brock et al., 2014b, and Brock and Xepapadeas, 2017b). A simpler approach is the use of the two-box energy balance model introduced by Langen and Alexeev (2007) and Alexeev and Jackson (2012). The model consists of a single hemisphere with two boxes or regions divided by the 30th latitude, which yields similar surface area of the two boxes. The two-box model of Langen and Alexeev (2007) with anthropogenic forcing is presented in Figure 1.

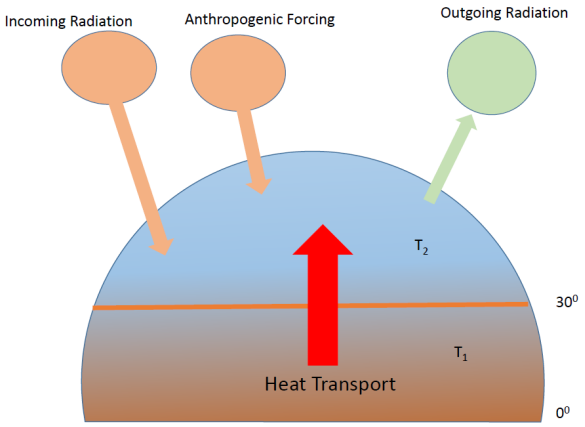

Figure 1. A two-box EBCM

Assuming no anthropogenic forcing, the evolution of the ocean mixed-layer temperature in each box is:

$$\dot{T}_{1T} = \frac{1}{H}\left(S_1 - A - BT_{1T} - Tr\right) \tag{1}$$

$$\dot{T}_{2T} = \frac{1}{H}\left(S_2 - A - BT_{2T} + Tr\right), \tag{2}$$

where T_{jT} , $j = 1, 2$ is the ocean mixed-layer temperatures in each region, with 1 denoting the South and 2 the North. This temperature is defined as the sum of equilibrium, or baseline, average temperature in each box (T_{1b}, T_{2b}) when anthropogenic forcing through emissions of GHGs is zero, plus the temperature anomaly (T_1, T_2). Thus the temperature anomaly in each region is defined as $T_j = T_{jT} - T_{jb}$, $j = 1, 2$. By the definition of the regions, the baseline average yearly temperatures (T_{1b}, T_{2b}) satisfy the inequality $T_{1b} > T_{2b}$. The downwelling shortwave radiation in each region is denoted by S_j, the outgoing longwave radiation by $A + BT_{jT}$, the heat transport from box 1 to box 2 by Tr, and the upper ocean layer heat capacity by H.

The meridional heat transport is defined in terms of the temperature anomaly as:

$$Tr = \bar{Tr} + \gamma_1 (T_1 - T_2) + \gamma_2 T_1. \tag{3}$$

In (3) the first term, $\bar{Tr}$, is the equilibrium heat transport, the second term captures the increase in transport due to increasing baroclinicity, while the third term captures the effect of an increased moisture supply and thus greater latent heat transport with increased low- to mid-latitude temperatures. To study the economics of climate change, anthropogenic forcing induced by emissions of GHGs should be introduced. The stock of GHGs created by anthropogenic emissions traps part of the outgoing longwave radiation.

In formulating the climate model, we seek a simplified representation which will allow us to derive some tractable results for cooperative and noncooperative equilibria. In widely-used integrated assessment models (IAMs) which couple the economy and the climate (e.g. DICE 2013-R, Nordhaus and Sztorc, 2013), the climate module represents a simplification of the more complex model used by climate science. In DICE 2013-R in particular, the carbon cycle is based upon a three-reservoir model, in which the reservoirs represent carbon in the atmosphere, the upper oceans and the deep oceans. Then the increase in radiative forcing, which induces an increase in the global mean temperature, is determined by the well-known relationship between the current concentration of CO_2 in the atmosphere and the preindustrial concentration in 1750 (see Nordhaus and Sztorc, 2013, pp. 16-17).

In this paper we employ a further simplification of the climate model (see for example Hassler et al., 2016, section 3.2.6; Brock and Hansen, 2017) which is based on climate literature developed over the last decade (Matthews et al., 2009; Matthews et al., 2012; Pierrehumbert, 2014). The simplification is based on linking emissions of CO_2 directly to changes in global mean temperature through the carbon-climate response (CCR), instead of linking CO_2 emissions to CO_2 concentration through carbon sensitivity and CO_2 concentration to changes in global mean temperature through climate sensitivity. The CCR is approximately constant and aggregates the climate and carbon sensitivities (including climate-carbon feedbacks) into a single metric representing the net temperature change per unit carbon emitted (MacDougall, 2016; Brock and Hansen, 2017, figure 2).

The relationship which is consistent with the observational record of global temperature change and anthropogenic CO_2 emissions has been named the transient climate response (TCRE) to CO_2 emissions (e.g. MacDougall et al., 2017). The TCRE embodies both the physical effect of CO_2 on climate and the biochemical effect of CO_2 on the global carbon cycle (Matthews et al., 2009). The TCRE, denoted by λ, is defined as $\lambda = \frac{\Delta T(t)}{CE(t)}$, where $CE(t)$ denotes cumulative carbon emissions up to time t and $\Delta T(t)$ the change in temperature during the same period. The constancy of λ suggests a linear

relationship between a change in global average temperature and cumulative emissions. This linear relationship has also been recognized by the IPCC (2013),[6], [7] while in the same context Knutti (2013) concludes that every ton of CO_2 causes about the same amount of warming, no matter when and where it is emitted.

MacDougall and Friedlingstein (2015) and MacDougall (2016) provide analytical arguments for the constancy of the TCRE over a relevant range of cumulative emissions of carbon.[8] MacDougall (2016, p. 42) states that:

> "... TCRE arises from a combination of (1) positive carbon-climate feedbacks increasing the airborne fraction of carbon; (2) weakening radiative forcing per unit CO_2 at higher atmospheric concentrations of CO_2; and (3) contributions from non-CO_2 radiative forcing. Notably without the contribution from non-CO_2 radiative forcing the simulated TCRE remains approximately constant until 1700 Pg C of CO_2 have been emitted to the atmosphere."

Using the definition of the TCRE in continuous time, the anthropogenic impact on the global temperature increase can be approximated by

$$T(t) - T(0) = \lambda \int_{s=0}^{t} E(s)\, ds \quad , \quad CE(t) = \int_{s=0}^{t} E(s)\, ds,$$

where $CE(t)$ denotes cumulative global carbon emissions up to time t and λ is the TCRE (see also Hassler et al., 2016, p. 1929). Taking the time derivative of the expression we obtain

$$\dot{T}(t) = \lambda E(t). \tag{4}$$

Using this approximation as a basis for our climate model,[9] let global

[6] In the IPCC (2013, p. 1113), it is stated that: "In conclusion, taking into account the available information from multiple lines of evidence (observations, models and process understanding), the near linear relationship between cumulative CO_2 emissions and peak global mean temperature is well established in the literature and robust for cumulative total CO_2 emissions up to about 2000 PgC. It is consistent with the relationship inferred from past cumulative CO_2 emissions and observed warming, is supported by process understanding of the carbon cycle and global energy balance, and emerges as a robust result from the entire hierarchy of models."

[7] Tokarska et al. (2016) report that, using simulations from four comprehensive Earth system models, the CO_2-attributable warming continues to increase approximately linearly up to 5 EgC emissions (an Eg (exagram) is a unit of mass equal to 10^{18} grams). These models simulate, in response to 5 EgC of CO_2 emissions, global mean warming of 6.4–9.5 °C, and mean Arctic warming of 14.7–19.5 °C.

[8] See MacDougall and Friedlingstein (2015, equations (10) and (11)), or MacDougall (2016, equations (7) and (8)).

[9] There are arguments pointing to the limitations of the TCRE concept and a number of questions to be answered (see MacDougall, 2016); however, it provides a simplified framework for studying climate problems, especially when optimal control and differential games tools are used.

emissions at each date t in the two-box model be defined as the sum of emissions in box 1, $E(1,t)$, and box 2, $E(2,t)$, or $E(t) = E(1,t) + E(2,t)$. Then, using Langen and Alexeev's (2007) parametrization and following Brock and Xepapadeas (2017a) in the linearity assumption, the anthropogenic impact can be expressed in terms of the evolution of the temperature anomaly in each box as:

$$\dot{T}_1 = \frac{1}{H}\left[(-B-\gamma_1-\gamma_2)T_1 + \gamma_1 T_2 + \lambda E(t)\right],\ T_1(0) = 0 \quad (5)$$

$$\dot{T}_2 = \frac{1}{H}\left[(\gamma_1+\gamma_2)T_1 + (-B-\gamma_1)T_2 + \lambda E(t)\right],\ T_2(0) = 0 \quad (6)$$

$$E(t) = [E(1,t) + E(2,t)]. \quad (7)$$

It is easy to show that with constant emissions $E(t)$, so that a steady state exists for (5)-(7), this steady state is determined as:

$$\bar{T}_1 = \frac{\lambda E(B+2\gamma_1)}{B(B+2\gamma_1+\gamma_2)}, \bar{T}_2 = \bar{T}_1 + \frac{2\lambda E\gamma_2}{B(B+2\gamma_1+\gamma_2)}.$$

When $\gamma_2 = 0$, the steady-state temperature anomaly between low and high latitudes is the same. On the other hand, in a steady state where $\gamma_2 > 0$, $\bar{T}_2 > \bar{T}_1$. Thus $\gamma_2 > 0$ in (3) breaks symmetry between the two regions if $E(t)$ is constant.

2.2 Surface Albedo Feedback

Another mechanism which induces AA is the surface albedo feedback (SAF). The SAF mechanism suggests that initial warming in the North Pole will melt some of the Arctic's highly reflective (high albedo) snow and ice cover. This will expose darker surfaces which will absorb solar energy, leading to further warming and further retreat of snow and ice cover. This process is presented in Figure 2.

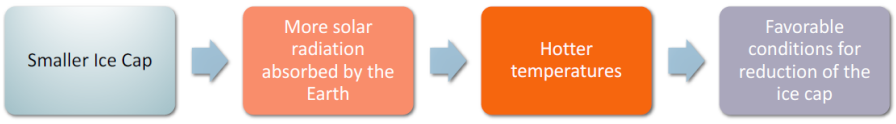

Figure 2. The surface albedo feedback (SAF)

As shown in Brock and Xepapadeas (2017a), a simple linear SAF mechanism can be incorporated into the two-box model describing heat transfer by writing the second term in the brackets of (6), which indicates heat dissipation in region 2, as $(-B-\gamma_1+\alpha_2 S_2)T_2$, where α_2 is a co-albedo coefficient.

In this case results suggest that when the SAF effect is added, region 2's temperature will be higher and thus any damage in region 1 caused by higher temperature in region 2 will be further augmented. So the linear SAF can be easily incorporated into the model by redefining the term $-B_1 - \gamma_1$ as $(-B_1 - \gamma_1 + \alpha_2 S_2)$, which means that heat dissipation slows down in region 2. Therefore, heat transfer warms the Arctic faster. As T_2 increases, T_1 increases as well, as indicated by the $\gamma_1 T_2$ terms in (5). This triggers more heat transfer and SAF which warms the Arctic even more.

Another type of feedback induced by AA could increase temperature in both regions through the release of GHGs as permafrost thaws under AA (see, for example, Schuur et al., 2015). This can be modelled by redefining total emissions as

$$E(t) = \left[E(1,t) + E(2,t) + E^P(T_2(t))\right],$$

where $E^P(T_2(t))$ is an increasing function of the temperature in the North, indicating GHGs emissions from permafrost. This function could be characterized by threshold effects and some upper bound on cumulative emissions from permafrost.[10]

3 Welfare Optimization

Using the temperature dynamics (5)-(7), we study optimal paths under cooperative and non-cooperative solutions. For the cooperative solution, global welfare is expressed by the sum of welfare in each region:

$$\int_{t=0}^{\infty} \mathrm{e}^{-\rho t} \left[\sum_{j=1}^{j=2} v(j) L(j,t) \ln\left[y(j,t) E(j,t)^{\alpha} \mathrm{e}^{-\phi(j,T_b+T)}\right]\right] dt, \qquad (8)$$

where $y(j,t) E(j,t)^{\alpha}$, $0 < \alpha < 1$, $E(j,t)$, $T_{bi}(j)$, $T_i(j,t)$ $L(j,t)$ are output per capita, fossil fuel input or emissions of GHGs, baseline temperature, temperature anomaly and fully employed population in each region j at date t, respectively. The term $\mathrm{e}^{-\phi(j,T_b+T)}$, $T_b + T = (T_{b1} + T_1, T_{b2} + T_2)$ reflects damages to output per capita in region $j = 1, 2$ from an increase in the temperature anomaly in either region, since AA in region 2 might generate damages to region 1.

By abstracting away from the problem of optimally accumulating capital inputs and other inputs, in order to focus sharply on optimal cooperative and non-cooperative fossil fuel taxes, we assume that $y(j,t)$, $L(j,t)$ are exogenously given. Thus, $y(j,t)$ could be interpreted as the component of a Cobb-Douglas production function which is a composite of all other inputs

[10] We do not model permafrost effects in this paper. This could be an interesting area for further research.

along with technical change that evolves exogenously. Finally, $v(j)$ represents welfare weights associated with each region. It should be noted that this is a stylized two-region model, specially designed to focus on sharply exposing the impact of heat and moisture transport from the South towards the North Pole, on cooperative and non-cooperative climate change policies. Therefore, by necessity some important economics are left out.[11,12] To simplify the exposition we assume that fossil fuels are abundant in both regions and provided at zero cost. The use of fossil fuels is, however, costly in terms of climate.

The current value Hamiltonian for maximizing (8) subject to temperature dynamics in each region and the resource constraints is:

$$\begin{aligned}
&\mathcal{H} = \\
&\sum_{j=1}^{j=2} \left\{ v(j) L(j) \left[\alpha \ln E(j,t) - \phi(j, T_b + T) \right] \right\} + \\
&\lambda_{T_1} \frac{1}{H} \left[(-B - \gamma_1 - \gamma_2) T_1 + \gamma_1 T_2 + \lambda \left[E(1,t) + E(2,t) \right] \right] + \\
&\lambda_{T_2} \frac{1}{H} \left[(\gamma_1 + \gamma_2) T_1 + (-B - \gamma_1) T_2 + \lambda \left[E(1,t) + E(2,t) \right] \right] \\
&T_b = (T_{b1}, T_{b2}) \ , \ T = (T_1, T_2) .
\end{aligned}$$

The optimality condition for the optimal fossil fuel path is:

$$\begin{aligned}
\frac{\alpha v(j) L(j)}{E(j,t)} &= \frac{-\lambda \left(\sum_{i=1}^{2} \lambda_{T_i}(t) \right)}{H} \ , \text{ or} \\
E(j,t) &= \frac{-\alpha v(j) L(j) H}{-\lambda \left(\sum_{i=1}^{2} \lambda_{T_i}(t) \right)} \ , \ j = 1, 2.
\end{aligned}$$

Thus, the externality tax associated with anthropogenic emissions of GHGs is determined as:

$$\tau(t) = \frac{-\lambda \left(\sum_{i=1}^{2} \lambda_{T_i}(t) \right)}{H}. \tag{9}$$

The externality tax is likely to increase as the cumulative carbon response parameter, λ, of Matthews et al. (2009) increases and the heat capacity H decreases.

[11] For example, we assume fixed initial fossil fuel reserves when they are evidently not fixed (e.g., shale gas). Furthermore the model has full exhaustion of reserves. For a more realistic but computationally intensive model, see Cai et al. (2017).

[12] We focus on the Northern Hemisphere because the geography is very different in the Southern Hemisphere, the PA is weaker there and, most importantly, most of the world's economic activity takes place north of the Equator. Evidence indicates that 88% of the global population lives in the Northern Hemisphere (http://www.radicalcartography.net/index.html?histpop).

3.1 Cross Region Damages and Optimality Conditions

To explore the impact of AA on both regions in a tractable way, the following assumption regarding marginal damages is made:

Assumption 1: *Define marginal damage cost of temperature increase in region* $i = 1, 2$ *by*

$$\begin{aligned} d_1 &= \left(d_{11}^0 + d_{12}^0\right) + d_{11}^1 T_1 + d_{12}^1 T_2 \\ d_2 &= \left(d_{21}^0 + d_{22}^0\right) + d_{21}^1 T_1 + d_{22}^1 T_2 \\ d_i &= \sum_{j=1}^{2} v\left(j\right) L\left(j\right) \frac{\partial \phi\left(i, T_b + T\right)}{\partial T_j} \; i = 1, 2, \end{aligned}$$

where the anomaly-related damage in each box is defined as

$$\begin{aligned} v\left(1\right) L(1) \phi\left(1, T_1, T_2\right) &= d_{11}^0 T_1 + (1/2) d_{11}^1 \left(T_1\right)^2 \\ &\quad + d_{12}^0 T_2 + (1/2) d_{12}^1 \left(T_2\right)^2 \\ v\left(2\right) L(2) \phi\left(2, T_1, T_2\right) &= d_{21}^0 T_1 + (1/2) d_{21}^1 \left(T_1\right)^2 \\ &\quad + d_{22}^0 T_2 + (1/2) d_{22}^1 \left(T_2\right)^2 . \end{aligned}$$

It is assumed that d_{ij}^l, $i, j = 1, 2$, $l = 0, 1$ *are constants at all dates.*

Thus, marginal damages in both regions from a change in temperature in region $i = 1, 2$ are:

$$\begin{aligned} \hat{d}_1 &= \left(d_{11}^0 + d_{21}^0\right) + \left(d_{11}^1 + d_{21}^1\right) T_1 = d_1^0 + d_1^1 T_1 \\ \hat{d}_2 &= \left(d_{12}^0 + d_{22}^0\right) + \left(d_{12}^1 + d_{22}^1\right) T_2 = d_2^0 + d_2^1 T_2. \end{aligned}$$

In Assumption 1, the parameters $\left(d_{21}^l, d_{12}^l\right)$, $l = 0, 1$ capture the cross effects from an increase in the temperature anomaly in one region on the damages of the other region. In particular, d_{12}^l, $l = 0, 1$ captures the effects of an increase in temperature in region 2, on damages in region 1. We will say that:

- AA effects in the sense of aggregate marginal damages are strong if $\left(d_2^0, d_2^1\right) > \left(d_1^0, d_1^1\right)$, and weak if $\left(d_2^0, d_2^1\right) < \left(d_1^0, d_1^1\right)$.
- An increase in temperature in region 2 will have a stronger impact in the South than the North if $\left(d_{12}^0, d_{12}^1\right) > \left(d_{22}^0, d_{22}^1\right)$, or $d_{12}^l > d_{22}^l, l = 0, 1$. This can be regarded as an indication that AA has stronger "remote effects" in region 1.
- An increase in temperature in region 2 will have a stronger impact in the North than the South if $\left(d_{12}^0, d_{12}^1\right) < \left(d_{22}^0, d_{22}^1\right)$, or $d_{12}^l < d_{22}^l, l = 0, 1$. This can be regarded as an indication that AA has stronger "local effects" in region 2.

The optimality conditions for the costate equations of the climate dynamics, setting without loss of generality $H = 1$, imply:

$$\dot{\lambda}_{T_1} = [\rho + (B + \gamma_1 + \gamma_2)]\,\lambda_{T_1} - (\gamma_1 + \gamma_2)\,\lambda_{T_2} + d_1^0 + d_1^1 T_1 \quad (10)$$

$$\dot{\lambda}_{T_2} = -\gamma_1 \lambda_{T_1} + [\rho + (B + \gamma_1)]\,\lambda_{T_2} + d_2^0 + d_2^1 T_2, \quad (11)$$

with steady-state values obtained by setting $\left(\dot{\lambda}_{T_1}, \dot{\lambda}_{T_2}\right) = (0, 0)$, or

$$\lambda_{T_1}^* = \phi_1 (T_1, T_2)\,,\ \lambda_{T_2}^* = \phi_2 (T_1, T_2)\,.$$

Then, the steady-state optimal carbon tax is defined, at $\left(\lambda_{T_1}^*, \lambda_{T_2}^*, T_1^*, T_2^*\right)$, as:

$$\tau^* = -\lambda \left[\phi_1 (T_1^*, T_2^*) + \phi_2 (T_1^*, T_2^*)\right]. \quad (12)$$

4 Bias from Ignoring Heat Transport

We are interested in calculating the error made if the planner mistakenly ignores heat transfer Tr in computing optimal carbon taxes. To calculate this error, we compute the solution by the planner who acts as if $Tr = 0$, but $Tr \neq 0$ is present in the actual climate. In terms of the model, ignoring heat transport is equivalent to setting $\gamma_1 = \gamma_2 = 0$. We denote by $\hat{\tau} = \tau (0, 0)$ the steady-state optimal carbon tax without heat transport and by $\tau (\gamma_1, \gamma_2)$ the steady-state optimal carbon tax under heat transport, i.e. $(\gamma_1, \gamma_2) \neq (0, 0)$. Then the bias from ignoring heat transport can be defined as:

$$\frac{\hat{\tau}}{\tau (\gamma_1, \gamma_2)} = \frac{\tau (0, 0)}{\tau (\gamma_1, \gamma_2)} \quad (13)$$

$$\hat{\tau} (0, 0) = \frac{\lambda \left[d_1^0 + d_2^0 + \left(d_1^1 + d_2^1\right) \hat{T}\right]}{(\rho + B)} \quad (14)$$

$$\tau^* (\gamma_1, \gamma_2) = \quad (15)$$
$$\left[(\rho + B + 2\gamma_1) \left(d_1^0 + d_2^0\right)\right.$$
$$\left. + 2 d_2^0 \gamma_2 + d_1^1 (B + 2\gamma_1 + \rho)\, T_1^* + d_2^1 (B + 2 (\gamma_1 + \gamma_2) + \rho)\, T_2^*\right] \div$$
$$\div \left[(\rho + B) (\rho + B + 2\gamma_1 + \gamma_2)\right],$$

where $\hat{T}$, (T_1^*, T_2^*) indicate the estimated global steady-state temperature when heat transport is ignored by the regulator, while (T_1^*, T_2^*) indicate the estimated steady-state temperatures for each region when the regulator takes into account heat transport.

The "gap" between the incorrect steady-state "optimal" tax rate and the correct tax rate depends on the steady-state levels of the global temperature and the regional anomalies. Therefore, in order to obtain some insights about the sign and the direction of the bias we resort to numerical simulations.

The values used in the simulations are described in detail in Brock and Xepapadeas (2017a). To explore numerically the bias and its direction from ignoring AA, we calculated the unique steady-state temperature anomaly when AA is not taken into account, the steady-state temperature anomalies in each region when AA is accounted for, and the corresponding ratios $\hat{\tau}/\tau^*$ using the damage parametrization $d_1^0 = 0.05$, $d_2^0 = \{0.01, 0.02, 0.04\}, d_1^1 = 0.01, d_2^1 = 0.005$, which corresponds to weak AA according to our definition, and $d_1^0 = 0.05$, $d_2^0 = \{\ 0.1, 0.15, 0.2\}\ , d_1^1 = 0.01, d_2^1 = 0.05$, which corresponds to strong AA. Figure 3 presents the ratio $\hat{\tau}/\tau^*$ for the different values of d_2^0.

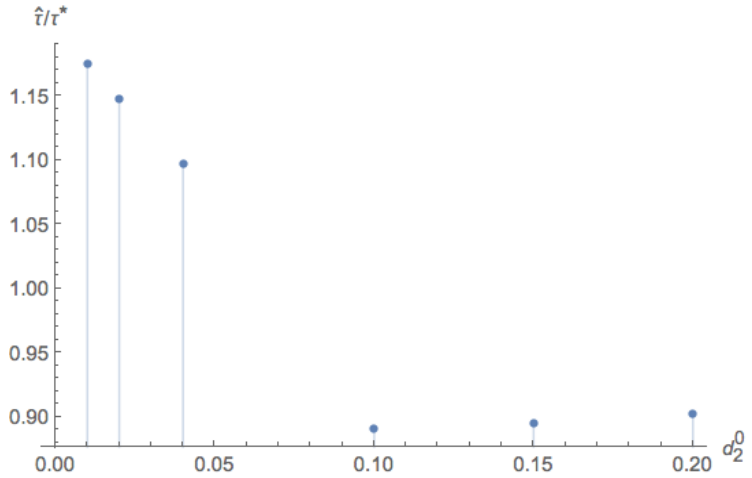

Figure 3. Tax bias from ignoring AA

The numerical results suggest that under weak AA effects, the "wrong optimal" steady-state tax $\hat{\tau}$, calculated by ignoring AA, exceeds the optimal tax τ^*, while the bias is in the opposite direction under strong AA.

4.1 Simulating the Temperature Paths

To obtain insights about the dynamic behavior of the optimal temperature paths, the modified dynamic Hamiltonian system resulting from the solution of problem (8) is linearized around the saddle point steady state, and then the system of four differential equations for the temperature anomalies and the corresponding costate variables is fully solved with and without heat transport. The evolution of temperature anomalies and the expected global anomaly without heat transport effects is shown in Figures 4-6.

Figure 4 depicts the optimal paths for the temperature anomalies in the two regions (boxes) under strong AA effects with $\left(d_2^0, d_2^1\right) = (0.2, 0.05) > \left(d_1^0, d_1^1\right) = (0.05, 0.01)$, along with the path for the global temperature calculated by a regulator who does not take AA into account. Figure 5 depicts the evolution of the paths of the temperature anomalies (T_{1W}, T_{2W}) which

will actually emerge, given the two-box dynamics of the climate system, when a regulator ignores AA and calculates an emission path which is based on misspecified climate dynamics. In this case an optimal emission path is determined without taking into account heat transport and AA. However, since heat transport and SAF is actually taking place in the real climate and the parameter γ_2 is positive, the climate system will generate separate paths for the regional anomalies, because there is heat transfer from region 1 to region 2 and then the temperature in region 2 has a positive effect on the rate of change in temperature in region 1 as indicated by (5). To determine these paths, the emission path obtained from the optimized system, *without heat transport*, was substituted into the temperature anomalies dynamics (5)-(6), and the system was solved with the "wrong planned emissions."

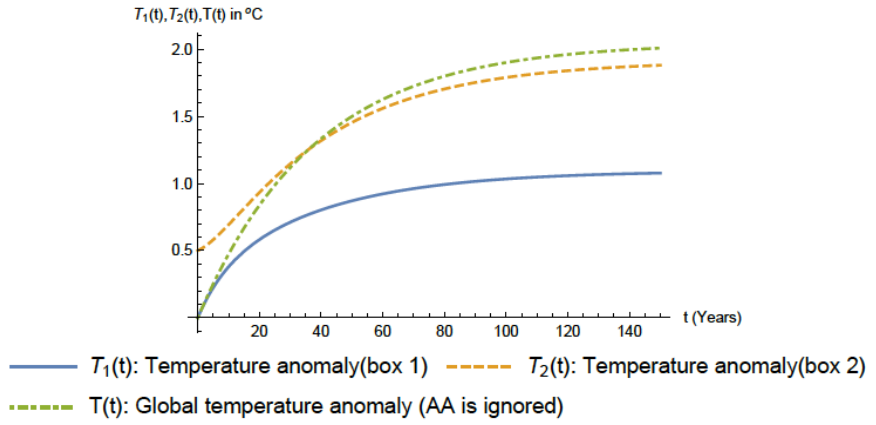

Figure 4. Regional and global temperature anomalies under strong AA

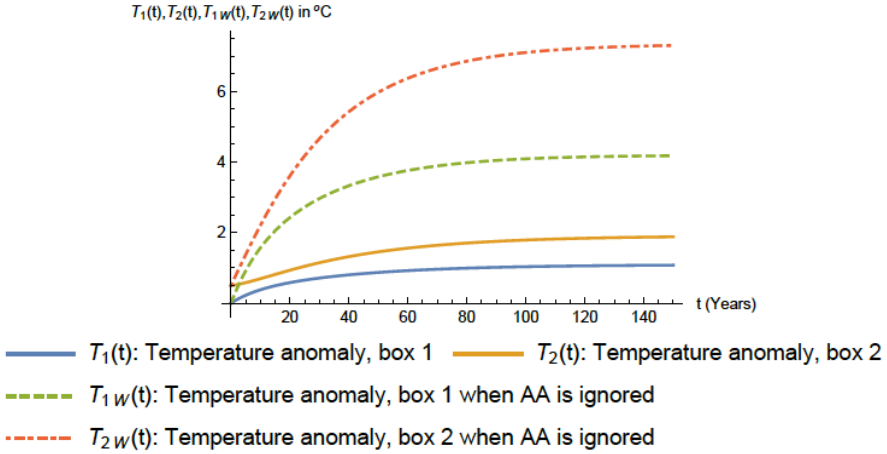

Figure 5. Evolution of temperature anomalies (T_{1W}, T_{2W}) with the wrong planned emissions relative to optimal anomalies under strong AA

The numerical simulations indicate that ignoring AA when it is actually present leads to higher emissions relative to the optimal paths and therefore the relatively higher temperature anomalies shown in Figure 5. Figures 6 and 7 provide similar results but with weak AA effects, or $\left(d_2^0, d_2^1\right) = (0.05, 0.01) < \left(d_1^0, d_1^1\right) = (0.2, 0.05)$.

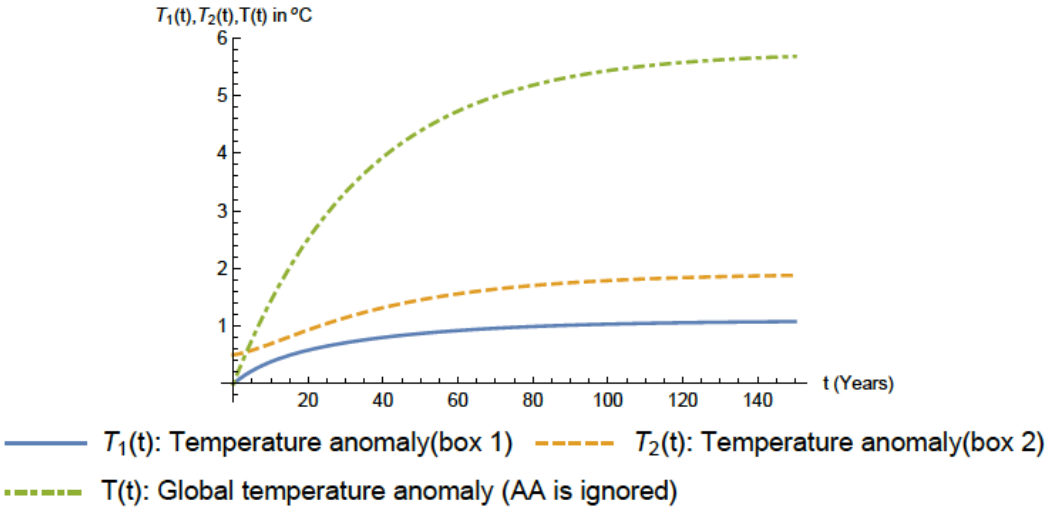

Figure 6. Regional and global temperature anomalies under weak AA

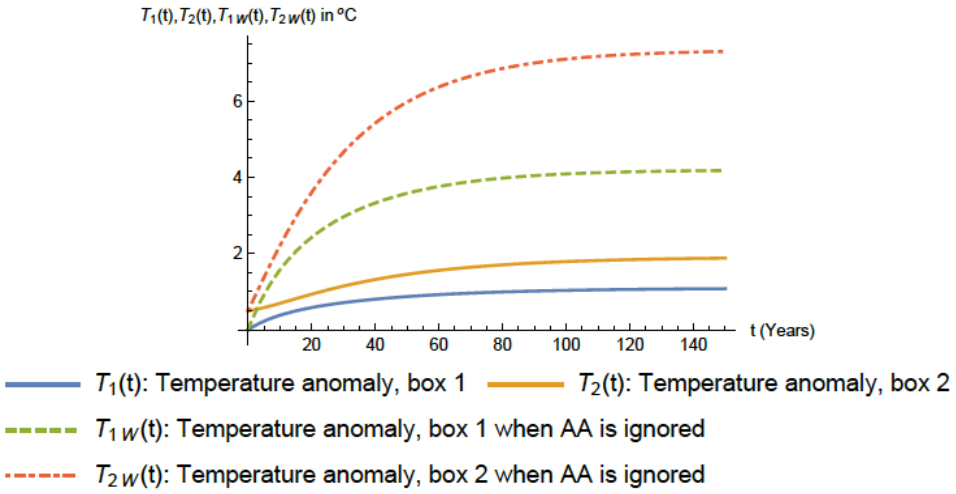

Figure 7. Evolution of temperature anomalies (T_{1W}, T_{2W}) with the wrong planned emissions relative to optimal anomalies under weak AA

Weak AA effects regarding damages lead to higher emissions and temperatures relative to strong AA effects. This is because when AA effects are

weak, incremental damages from the relatively higher temperature in the North, due to AA, tend to be lower relative to the strong AA.

It is clear that whether AA effects are strong or weak is an empirical issue. The analysis suggests, however, that using the "wrong planned emissions" will result in suboptimal regional temperature anomalies relative to the optimal anomalies. This result could have significant policy implications since it implies that if heat transport and related feedbacks are not taken into account, the planned emissions will be suboptimal, and this will lead to higher than desired regional temperatures.

5 Welfare Effects

Suppose that the planner mistakenly believes that heat and moisture transport is not present, i.e. $(\gamma_1, \gamma_2) = (0, 0)$, but the true dynamics are $\gamma_1 > 0, \gamma_2 > 0$. How big is the error in welfare units and how big is the error in energy use and emissions taxes?

A proportional welfare gain for each region by accounting for AA can be defined as:

$$\psi(j) = \frac{W[j, (\gamma_1, \gamma_2) \mid (\gamma_1, \gamma_2)] - W[j, (a_1, a_2) \mid (\gamma_1, \gamma_2)]}{W[j, (a_1.a_2) \mid (\gamma_1, \gamma_2)]}\ ,\ j = 1, 2, \quad (16)$$

as a measure of the error made by a planner who believes $(a_1.a_2)$ when the true parameters are (γ_1, γ_2).

$$W[j, (\gamma_1, \gamma_2) \mid (\gamma_1, \gamma_2)] = \quad (17)$$
$$\int_{t=0}^{\infty} \mathrm{e}^{-\rho t} [v(j) L(j,t) \times$$
$$\ln \left[y(j,t) E(j, t \mid (\gamma_1, \gamma_2))^{\alpha} \mathrm{e}^{-\phi(j, T(\gamma_1, \gamma_2))} \right] dt$$
$$W[(a_1, a_2) \mid (\gamma_1, \gamma_2)] = \quad (18)$$
$$\int_{t=0}^{\infty} \mathrm{e}^{-\rho t} [v(j) L(j,t) \times$$
$$\ln \left[y(j,t) E(j, t \mid (a_1, a_2))^{\alpha} \mathrm{e}^{-\phi(j, T(a_1, a_2))} \right] dt$$
$$(a_1, a_2) = (0, 0)\ ,\ j = 1, 2, \quad (19)$$

where $T(a_1, a_2) = (T_1(a_1, a_2), T_2(a_1, a_2))$ are the anomalies emerging from using the emissions paths derived from welfare optimization without heat transport and AA effects.

The simulation results, using a terminal time of $t = 1000$ for the numerical integration, indicate that:

a.

$$\psi(1) = 31.0\% \tag{20}$$
$$\psi(2) = 32.1\%, \tag{21}$$

when an increase in temperature in region 2 has stronger "local effects" in the North than the South or $d_{12}^l < d_{22}^l$, $l = 0, 1$. This can be regarded as an indication that AA is stronger in region 2.

b.

$$\psi(1) = 31.6\% \tag{22}$$
$$\psi(2) = 31.5\%, \tag{23}$$

when an increase in temperature in region 2 has stronger "remote effects" in the South than the North or $d_{12}^l > d_{22}^l$, $l = 0, 1$.

This result is another indication of potential suboptimal outcomes when heat transport and AA are ignored.

6 Non-Cooperative Solutions

6.1 Open Loop Nash Equilibrium (OLNE)

In a non-cooperative world, each region chooses emissions paths to maximize own welfare, taking the emissions path of the other region as given, or:

$$\max_{E(j,t)} J(j), \ j = 1, 2 \tag{24}$$
$$J(j) = \int_{t=0}^{\infty} \mathrm{e}^{-\rho t} \left[v(j) L(j,t) \ln \left[y(j,t) E(j,t)^{\alpha} \mathrm{e}^{-\phi(j, T_b + T)} \right] \right] dt,$$

subject to temperature dynamics and resource constraints. It is assumed that each region follows open loop strategies by committing to emissions paths at the beginning of the time horizon. Then, the solution of problem (24) using the maximum principle will provide the open loop Nash equilibrium (Basar and Olsder, 1995).

The current value Hamiltonian for each region is:

$$\begin{aligned}
&\mathcal{H}_j^{OL} = \\
&v(j) L(j) \left[\alpha \ln E(j,t) - \phi(j, T_b + T) \right] + \\
&\lambda_{jT_1}^{OL} \frac{1}{H} \left[(-B - \gamma_1 - \gamma_2) T_1 + \gamma_1 T_2 + \lambda \left[E(j,t) + \bar{E}(i,t) \right] \right] + \\
&\lambda_{jT_2}^{OL} \frac{1}{H} \left[(\gamma_1 + \gamma_2) T_1 + (-B - \gamma_1) T_2 + \lambda \left[E(j,t) + \bar{E}(i,t) \right] \right] \\
&T_b = (T_{b1}, T_{b2}) \ , \ T = (T_1, T_2), j \neq i, \ j = 1, 2.
\end{aligned}$$

The optimality conditions for the costate equations of the climate dynamics, setting without loss of generality $H = 1$, imply:

$$\begin{aligned}\dot{\lambda}_{jT_1}^{OL} &= [\rho + (B + \gamma_1 + \gamma_2)]\,\lambda_{jT_2}^{OL} - (\gamma_1 + \gamma_2)\,\lambda_{jT_2}^{OL} + d_{j1}^0 + d_{j1}^1 T_1 \\ \dot{\lambda}_{jT_2}^{OL} &= -\gamma_1 \lambda_{jT_2}^{OL} + [\rho + (B + \gamma_1)]\,\lambda_{jT_2}^{OL} + d_{j2}^0 + d_{j2}^1 T_2\ ,\ j = 1, 2.\end{aligned}$$

Given that the regions are not symmetric with respect to damages, the costates are not the same and the externality tax is different between regions. The asymmetry depends on the damage parameters. This is because in the cooperative solution the social planner takes into account damages to both regions from a change of temperature in one region, while in the non-cooperative solution each region considers damages to itself only. The structure of marginal damages in the cooperative and the non-cooperative cases are shown below.

Cooperative
$\Delta T_1 : d_1^l = d_{11}^l + d_{21}^l, l = 0, 1\ , \Delta T_2 : d_2^l = d_{12}^l + d_{22}^l\ ,\ l = 0, 1$
Non-cooperative
Region 1: $\Delta T_1 : d_{11}^l$, $\Delta T_2 : d_{12}^l\ ,\ l = 0, 1$
Region 2: $\Delta T_1 : d_{21}^l$, $\Delta T_2 : d_{22}^l\ ,\ l = 0, 1$

With regional steady-state values at $\left(\dot{\lambda}_{jT_1}^{OL}, \dot{\lambda}_{jT_2}^{OL}\right) = (0, 0)$, the steady-state optimal externality taxes at OLNE are

$$\tau_j^* = -\lambda \left[\lambda_{jT_1}^{*OL} + \lambda_{jT_2}^{*OL}\right]. \tag{25}$$

Solving the non-symmetric OLNE and then linearizing the Hamiltonian systems around the OLNE steady states, we obtain the OLNE paths for the temperature anomalies and the corresponding costate variables. The costate variables provide an estimate of the climate externality in each region from a change in temperature in the North or the South. As expected, under OLNE the temperature anomalies are higher and the cost of climate externality lower relative to the cooperative solution.

Table 1 presents steady-state comparisons between the cooperative solution and OLNE. Notice that in the non-cooperative solutions, the existence of "local" $d_{12}^l < d_{22}^l$, or "remote" $d_{12}^l > d_{22}^l$ damage effects from an increase in temperature in region 2 makes a difference in the results of the non-cooperative equilibrium, but not in the cooperative because the social planner takes into account the sum of these damage parameters. Because of this discrepancy, the existence of local or remote effects are important for the properties of non-cooperative equilibria. If the effects are remote, then the higher anomaly in the North is associated with lower marginal damages and this induces relatively more emissions and eventually higher temperature in both regions relative to the case of local effects.

Table 1. Steady-state comparisons: Cooperative, OLNE

Equilibrium	Temperature 1	Temperature 2	Costate 1	Costate 2
Cooperative:	$T_1 : 1.09$	$T_2 : 1.91$	$\lambda^*_{T_1} : -4.08$	$\lambda^*_{T_2} : -5.76$
OLNE $d^l_{12} < d^l_{22}$:	$T_1 : 1.85$	$T_2 : 3.23$	$\lambda^{*OL}_{1T_1} : -2.19$ $\lambda^{*OL}_{2T_1} : -2.73$	$\lambda^{*OL}_{1T_2} : -2.84$ $\lambda^{*OL}_{2T_2} : -4.18$
OLNE $d^l_{12} > d^l_{22}$:	$T_1 : 1.90$	$T_2 : 3.34$	$\lambda^{*OL}_{1T_1} : -3.14$ $\lambda^{*OL}_{2T_1} : -1.82$	$\lambda^{*OL}_{1T_2} : -4.39$ $\lambda^{*OL}_{2T_2} : -2.70$

Table 1 suggests that the optimal externality tax in each region will be lower than the cooperative tax because each region takes into account own damages. A social planner seeking to implement the cooperative tax needs to impose an additional tax in each region. This additional tax should bridge the gap between the optimal tax under full cooperation and the regional OLNE taxes, and is defined below, for the case of the steady-state tax.

$$\tau^{*OPT}_j = -\lambda \left[\lambda^*_{T_1} + \lambda^*_{T_2}\right] - \left(-\lambda \left[\lambda^{*OL}_{jT_1} + \lambda^{*OL}_{jT_2}\right]\right), \text{ Region } j = 1, 2. \quad (26)$$

There are welfare gains from moving to the cooperative equilibrium which are shown in Table 2.

Table 2. Welfare gains (%) from moving from OLNE to full cooperation

Region 1	$d^l_{12} < d^l_{22}$	48.9%	$d^l_{12} > d^l_{22}$	51.6%
Region 2		50.3		51.5

6.2 Feedback Nash Equilibrium (FBNE)

As is well known, the OLNE is weakly time-consistent but not strongly time-consistent (Basar, 1989), that is, it does not possess the Markov perfect property and is not robust against unexpected changes in the state of the system. Therefore, the feedback Nash equilibrium (FBNE) is considered to be a more satisfactory solution concept. It is derived in a dynamic programming framework, so that controls depend on the state, and the solution is Markov perfect by construction. To obtain a strong time-consistent noncooperative equilibrium, we resort to feedback strategies. It is assumed that each region follows non-symmetric time stationary FBNE emission strategies of the form

$$E_j = h_j\left(T_1, T_2\right). \quad (27)$$

Since the anomalies in both regions affect the regions' welfare, it is natural to assume that each region's feedback rule will depend on both anomalies.

To obtain tractable solutions, the problem is transformed into a linear quadratic (LQ) problem. In a concave LQ problem with linear feedback

strategies, the FBNE stock of GHGs should be above the OLNE. Since we have two states, one would expect the FBNE steady state with linear strategies to be in the northeastern quadrant of the OLNE, in terms of our problem. However, we cannot determine the FBNE steady state unless we know the strategies, but we cannot know the strategies unless we solve the problem. If we have an LQ problem, then the Hamilton-Jacobi-Bellman (HJB) equation with a quadratic value function can be used to fully identify the feedback strategies and the steady state.[13] To provide an LQ representation of our problem, we note that dynamics are linear and the only nonlinearity exists in the objective function through the $\ln E(j,t)$, $j=1,2$, since the damage functions are quadratic. Thus, we expand the $\ln E(j,t)$ function by taking a second order Taylor approximation around the OLNE steady state obtained in the previous section from the nonlinear representation. The LQ representation is then used to solve for the FBNE.[14]

Under the LQ representation, the HJB equation for each region becomes

$$\begin{aligned}
\rho V^j(T_1,T_2) &= \max_{q_j}\left[v(j)L(j)\left[w_{0j}+w_{1j}E_j+w_{2j}E_j^2-\phi(j,T_b+T)\right]\right.\\
&\quad +V^j_{T_1}\frac{1}{H}\left[(-B-\gamma_1-\gamma_2)T_1+\gamma_1 T_2+\lambda\left[q_j+h_i(T_1,T_2)\right]\right]\\
&\quad \left.+V^j_{T_2}\frac{1}{H}\left[(\gamma_1+\gamma_2)T_1+(-B-\gamma_1)T_2+\lambda\left[q_j+h_i(T_1,T_2)\right]\right]\right]\\
j,i &= 1,2, j\neq i.
\end{aligned}$$

Given the LQ structure of the problem, we consider quadratic value functions

$$V^j(T_1,T_2)=\upsilon_{0j}+\upsilon_{1j}T_1+\upsilon_{2j}T_2+\upsilon_{3j}T_1^2+\upsilon_{4j}T_2^2+\upsilon_{5j}T_1T_2\ ,\ j=1,2.$$

6.3 Solution

The solution involves the following steps:

1. Standard optimization determines emission strategies as linear feedback rules of the temperature anomalies. Since regions are asymmetric regarding damages, the two value functions have different parameters. Thus the FBNE is determined by a system of two value functions.

2. Substituting the feedback rules into the HJB, and collecting terms of the same power, a nonlinear system in the twelve unknown parameters

[13] Nonlinear strategies may also exist but, for a two-state asymmetric differential game, determining these strategies involves numerical analysis which is beyond the purpose of the present paper.

[14] To make sure that the LQ representation provides adequate results, we solved for the OLNE using the LQ representation and compared the results with the OLNE obtained from the nonlinear representation. It turns out that the steady states of each representation are very close to each other, paths to the ready states are similar, and the stability properties are the same.

of the value function $(v_{01}, v_{j1}, v_{j2}, v_{j3}, v_{j4}, v_{j5})$, $j = 1, 2$ is determined. Solution of this system provides the parameters of the value function.

To obtain some insights into the solution, we calculate the parameters numerically using the same parametrizations as in the cooperative and OLNE cases, and we distinguish as in the OLNE two cases of "local" $d_{12}^l < d_{22}^l$, or "remote" $d_{12}^l > d_{22}^l$, $l = 0, 1$, damage effects from an increase in temperature in region 2. The results can be summarized as follows:

- The value functions in both cases are concave.
- The linear feedback stategies have the expected negative slope with respect to regional temperatures, or

$$\begin{array}{lll} \text{Region 1} & d_{12}^l < d_{22}^l : & 0.166026 - 0.000471T_1 - 0.000783T_2 \\ & d_{12}^l > d_{22}^l : & 0.112236 - 0.000209T_1 - 0.000347T_2 \\ \text{Region 2} & d_{12}^l < d_{22}^l : & 0.124123 - 0.000177T_1 - 0.000230T_2 \\ & d_{12}^l > d_{22}^l : & 0.187453 - 0.000412T_1 - 0.000535T_2. \end{array} \tag{28}$$

- Substituting the feedback strategies into temperature dynamics, we obtain the evolution of the temperature anomalies at the FBNE. The steady states are:[15]

$$\begin{aligned} d_{12}^l &< d_{22}^l : T_1^{*FB} = 3.48, T_2^{*FB} = 6.10 \\ d_{12}^l &> d_{22}^l : T_1^{*FB} = 3.61, T_2^{*FB} = 6.31. \end{aligned}$$

These steady states are stable, as shown in the phase diagrams (Figures 8 and 9).

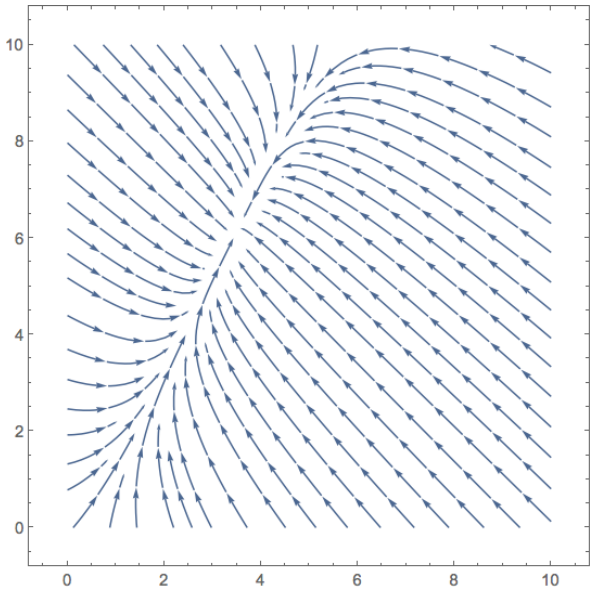

[15] As expected, these steady states are higher than the corresponding OLNE steady states resulting from both the original nonlinear and the LQ representations.

Figure 8. FBNE steady state when $d_{12}^l < d_{22}^l$

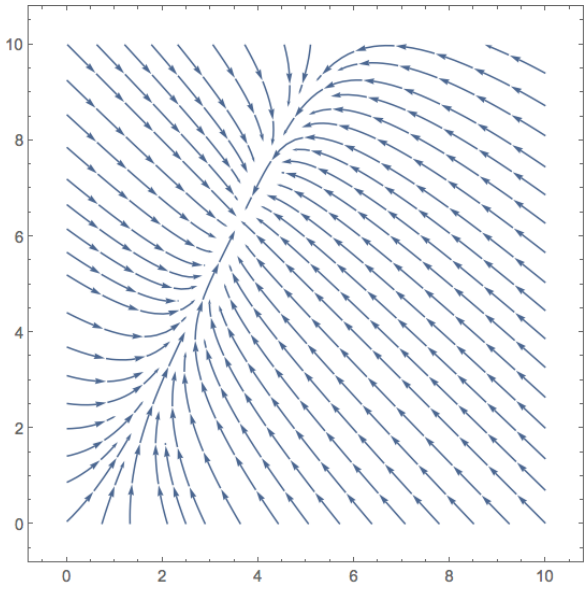

Figure 9. FBNE steady state when $d_{12}^l > d_{22}^l$

- In terms of welfare comparisons:
  - When $d_{12}^l < d_{22}^l$, the SWF in region 1 is 8.1% higher than in region 2.
  - When $d_{12}^l > d_{22}^l$, the SWF in region 2 is 23.6% higher than in region 1.

To interpret these results, note that if $d_{12}^l < d_{22}^l$, an increase in temperature in region 2, say due to AA, is expected to increase damages in the same region more than in region 1. On the other hand, if $d_{12}^l > d_{22}^l$, AA in region 2 generates more damages in region 1. In a sense, damages are "exported" and this can be related to extreme weather phenomena in the South due to AA or sea level rise emerging in the North which will damage the South. Thus when damages from AA are "exported", region 2 experiences higher welfare than region 2 and vice versa. Table 3 summarizes steady-state results from all three types of equilibria examined in this paper.

Table 3. Steady-state comparisons: Cooperative, OLNE, FBNE*

Equilibrium	Temperature 1	Temperature 2	Costate 1	Costate 2
Cooperative:	$T_1 : 1.09$	$T_2 : 1.91$	$\lambda^*_{T_1} : -4.08$	$\lambda^*_{T_2} : -5.76$
OLNE $d^1_{12} < d^1_{22}$:	$T_1 : 1.85$	$T_2 : 3.24$	$\lambda^{*OL}_{1T_1} : -2.19$	$\lambda^{*OL}_{1T_2} : -2.84$
			$\lambda^{*OL}_{2T_1} : -2.73$	$\lambda^{*OL}_{2T_2} : -4.18$
OLNE $d^1_{12} > d^1_{22}$:	$T_1 : 1.90$	$T_2 : 3.33$	$\lambda^{*OL}_{1T_1} : -3.14$	$\lambda^{*OL}_{1T_2} : -4.39$
			$\lambda^{*OL}_{2T_1} : -1.82$	$\lambda^{*OL}_{2T_2} : -2.70$
FBNE $d^1_{12} < d^1_{22}$:	$T_1 : 3.54$	$T_2 : 6.20$	$\lambda^{*FB}_{1T_1} : -6.409$	$\lambda^{*FB}_{1T_2} : -9.376$
			$\lambda^{*FB}_{2T_1} : -3.984$	$\lambda^{*FB}_{2T_2} : -4.651$
FBNE $d^1_{12} > d^1_{22}$:	$T_1 : 5.41$	$T_2 : 9.69$	$\lambda^{*FB}_{1T_1} : -6.534$	$\lambda^{*FB}_{1T_2} : -9.582$
			$\lambda^{*FB}_{2T_1} : -4.118$	$\lambda^{*FB}_{2T_2} : -4.799$

* In the two FBNE rows, the derivatives of the value functions with respect to the state variables are denoted by $\lambda^{FB}_{iT_i}, i = 1, 2$, instead of the usual $V^{*FB}_{iT_i}$, $i = 1, 2$ and are called costates in order to be homogeneous with the rest of the table.

The steady-state comparisons in Table 3 confirm the intuition that the FBNE will have higher regional temperatures and higher climate externality costs, as indicated by the values of the costate variables, than both the cooperative solution and the OLNE. The paths for the costate variables start from negative initial values and converge uniformly to their steady-state values. So the cost of the climate externality can be calculated at each point in time. The case in which incremental damages in region 1 from an increase in temperature in region 2 are higher than the corresponding damages in region 2, i.e. $d^l_{12} > d^l_{22}$ – the case or remote effects – could be of interest. This is because in this case there is a "flow" of damages from upstream to downstream and region 2, following either open loop or feedback rules, seems to have incentives to increase its emissions since part of the damages will be realized in region 1. This results in relatively higher steady-state anomalies both in OLNE and FBNE.

It should be finally noted that LQ differential games with feedback information structure could also have nonlinear feedback strategies (Dockner and van Long, 1993; Rowat, 2007). A nonlinear feedback strategy for our problem may lead to an equilibrium with different characteristics than the one obtained by linear strategies. Looking for nonlinear strategies is beyond the scope of the present paper. However, this is a potentially interesting area of further research, since the behavior of regions which may expect that part of the damages generated by their emissions will be borne by other regions can be explored in a model with non-cooperative behavior and spatial structure. This is not the case usually studied by the traditional IAMs of climate

change, which concentrate mainly on global mean temperature.[16]

As in the case of OLNE, a social planner seeking to implement the cooperative tax needs to impose an additional tax in each region. This additional tax should bridge the gap between the optimal tax under full cooperation and the regional FBNE value of the climate externality, so that

$$\tau_j^{*OPT} = -\lambda \left[\lambda_{T_1}^* + \lambda_{T_2}^*\right] - \left(-\lambda \left[\lambda_{jT_1}^{*FB} + \lambda_{jT_2}^{*FB}\right]\right), \text{ Region } j = 1, 2. \quad (29)$$

7 Two-Box Ramsey Type Models

This section develops a Ramsey-type modeling in the context of the two-region climate models of Alexeev and Jackson (2012) and Langen and Alexeev (2007). We continue to make rather drastic simplifying assumptions in order to concentrate on the impact of heat transport.

In developing the Ramsey model, we explicitly consider a Cobb-Douglas production function in each region,

$$Y(j,t) = A(j,t)\, K(j,t)^{\alpha_K}\, L(j,t)^{\alpha_L}\, E(j,t)^{\alpha_E} \ , \ j = 1, 2, \quad (30)$$

where $K(j,t)$ is the stock of capital and $A(j,t)$ is a productivity factor. Using this production function, the capital budget constraint for each region becomes

$$\dot{K}(j,t) = Y(j,t) - C(j,t) - \delta K(j,t) \ , \ j = 1, 2. \quad (31)$$

A deterministic Ramsey two-region optimization model is developed, which will be referred to as the "closed economy" problem. In this model, each region is limited by its own budget constraint and no transfers between regions take place. The particular assumptions connected to this scenario are restrictive and perhaps not so realistic, but they help to set up a benchmark model that can be compared with the other polar case in which the economy is completely open, with free flows of capital, fossil fuel and consumption goods across locations.

Assuming that utility in each region is logarithmic in effective consumption $Ce^{-\phi(j,T_b+T)}$, the current value Hamiltonian for this Ramsey-type problem is:

[16] The case where actions related to climate in one region could cause relatively more damages in other regions, when regions behave in a non-cooperative way, could also be interesting to study in the case of unilateral Solar Radiation Management (SRM). In this case unilateral SRM in one region could generate relatively higher damage through, for example, change in precipitation patterns, or acidification, in other regions. This could provide further incentives for unilateral SRM.

$$
\begin{aligned}
\mathcal{H} \;=\; & \sum_{j=1}^{j=2} \{v\left(j\right) L\left(j,t\right) \left[\ln C\left(j,t\right) - \phi\left(j, T_b + T\right)\right] + \\
& \lambda_{T_1}\left(t\right) \frac{1}{H} [\left(-B - \gamma_1 - \gamma_2\right) T_1 + \gamma_1 T_2 + \\
& \lambda \left[E\left(1,t\right) + E\left(2,t\right)\right]] + \\
& \lambda_{T_2}\left(t\right) \frac{1}{H} [\left(\gamma_1 + \gamma_2\right) T_1 + \left(-B - \gamma_1\right) T_2 + \\
& \lambda \left[E\left(1,t\right) + E\left(2,t\right)\right]] + \\
& \sum_{j=1}^{j=2} \lambda_K\left(j,t\right) \left[Y\left(j,t\right) - C\left(j,t\right) - \delta K\left(j,t\right)\right].
\end{aligned}
$$

In order to be able to study steady states, we make the simplifying assumptions constant population and no productivity growth in each region so that $L\left(j,t\right) = L\left(j\right), A\left(j,t\right) = A\left(j\right)$. Under these simplifying assumptions, the optimality condition for the two-region Ramsey model can be written as follows. For the controls $C(j,t), E\left(j,t\right)$:

$$
\begin{aligned}
\frac{v\left(j\right) L\left(j\right)}{C(j,t)} &= \lambda_K\left(j,t\right) \text{ or } C^0(j,t) = \frac{\alpha v\left(j\right) L\left(j\right)}{\lambda_K\left(j,t\right)} && (32)\\
\left(\lambda_{T_1}\left(t\right) + \lambda_{T_2}\left(t\right)\right) \frac{\lambda}{H} &= -\lambda_K\left(j,t\right) Z\left(j\right) \alpha_E K\left(j,t\right)^{\alpha_K} E\left(j,t\right)^{a_E - 1} && (33)\\
\text{or } \; E^0\left(j,t\right) &= \left[\frac{-\left(\lambda_{T_1}\left(t\right) + \lambda_{T_2}\left(t\right)\right)\left(\lambda/H\right)}{\lambda_K\left(j,t\right) Z\left(j\right) \alpha_E K\left(j,t\right)^{\alpha_K}}\right]^{\frac{1}{a_E - 1}} && (34)\\
Z\left(j\right) &= A\left(j\right) L\left(j\right)^{\alpha_L}. && (35)
\end{aligned}
$$

The complexity of the resulting Hamiltonian system does not allow analytical results. Therefore, some insights are obtained by resorting to simulations. For the climate system the parameters of the previous sections are used, while for the production system the following values are used:

$$
\alpha_K = 0.35, a_L = 0.60, a_E = 0.05, A(1) = A(2) = 1, \delta = 0.05. \tag{36}
$$

Steady-state results for the cooperative solution and the OLNE are shown below. All steady states have the saddle point property and the steady state externality tax is defined as $\tau = -\left(\lambda_{T_1} + \lambda_{T_2}\right) \frac{\lambda}{H}$.

Cooperative Solution: Steady states and externality tax (ET, \$/tCO$_2$)

T_1	T_2	λ_{T_1}	λ_{T_2}	ET
0.95	1.66	−3.92	−5.52	52.51

OLNE: Steady states and externality tax (ET, \$/tCO$_2$) and welfare gain (WG) from moving to the cooperative solution

$(d_{12} < d_{22})$

T_1	T_2	λ_{1T_1}	λ_{1T_2}	λ_{2T_1}	λ_{2T_2}	ET_1	ET_2	WG_1	WG_2
1.63	2.85	−2.09	−2.69	−2.58	−3.95	26.54	36.32	16%	36.4%

$(d_{12} > d_{22})$

T_1	T_2	λ_{1T_1}	λ_{1T_2}	λ_{2T_1}	λ_{2T_2}	ET_1	ET_2	WG_1	WG_2
2.27	3.98	−3.86	−4.76	−1.11	−1.49	45.33	14.48	237%	47.3%

At the OLNE, the additional tax in each region which is necessary to attain the cooperative steady state is ET - $\mathrm{ET}_j, j = 1, 2$.

8 Conclusions

An important characteristic of climate feedbacks is the transfer of heat from the equator to the Poles. When extra forcing through anthropogenic emissions is present, this transfer creates Polar or Arctic amplification. AA in turn could induce a "flow of damages" from the Poles to the South. In the present paper, a two-box – or two-region – climate model, which allows for heat and moisture transport from the southern region to the northern region, is coupled with an economic model of welfare optimization.

In the economic model, fossil fuel use or emissions are determined at cooperative and non-cooperative solutions. Non-cooperative solutions correspond to open loop and feedback Nash equilibrium solutions for the two regions. Non-cooperative solutions are asymmetric. Asymmetries stem from the differentiation of damages in each region due to AA.

Using numerical simulations, it is shown, in line with previous findings, that ignoring spatial heat and moisture transport and the resulting AA results in welfare loss and bias in a tax on GHG emissions. The results hold both for cooperative and non-cooperative solutions. The effects are, however, asymmetric and depend on which region suffers higher damages from AA.

When damages from AA are higher in region 1 than in region 2, results suggest that at a non-cooperative solution, region 2 has an incentive to increase emissions, especially when feedback strategies are followed, since a part of these damages move "downstream" to region 1.

The asymmetric behavior of regions at the non-cooperative solutions suggest that when each region follows a climate policy maximizing its own welfare, then different additions to regional carbon taxes should be applied if the objective is to attain the cooperative paths for emissions and temperature anomalies. The results remain robust when the model is extended to cooperative and OLNE solutions of a Ramsey-type growth model with heat transfer and AA.

Regarding the numerical estimates which provide the main quantitative insights, the present model – like many stylized abstract models – is meant only to be suggestive of what a more realistic exercise might find. Complex

models, like most of the IAMs, are difficult to comprehend, especially regarding the emergence of the numerical results (van der Ploeg and Rezai, 2016). On the other hand, relatively simple models could provide a framework in which the theoretical predictions seem to be confirmed by the numerical exercises.

The present model could be extended along different lines. The spatial structure could be enhanced by allowing for more regions, stochastic shocks could be introduced, and more advanced computational methods could be applied to solve the nonlinear feedback problem instead of using its linear-quadratic approximation. One of the most important issues, however, in this type of spatial modeling is the adequate estimation of regional damages. This is a crucial area for further research which will provide credibility to the quantitative estimates obtained from the models. For example, if heat transfer from the Equator to the Poles did not exist, damages from extreme heat documented by Hsiang et al. (2017) in the low latitudes might be even larger and mortalities from both extreme heat in the low latitudes and extreme cold in the high latitudes documented by Gasparrini et al. (2015) might be even larger. In this sense, heat transfer tends to reduce damages in the South. On the other hand, heat transport from low latitudes to high latitudes might affect the frequency and intensity of extreme weather events (Francis and Vavrus, 2014; Francis and Skific, 2015), and increase sea level rise, permafrost melt and climate tipping risks causing damages in the low latitudes with additional effects on carbon taxes and temperatures. Detailed work on estimating marginal temperature and damage impacts due to Equator-to-Pole heat transport will be needed in order to compute its overall impact on optimal policy.

Another important area of future research is to exploit recent work on emulation of responses of Atmospheric Ocean General Circulation Models (AOGCMs) in order to improve modeling of the climate dynamics component of our model. For example, Castruccio et al. (2014) fit the equation

$$\begin{aligned} T_t &= \beta_0 + \beta_1 \frac{1}{2}\left[\ln\frac{CO_{2,t}}{CO_{2,0}} + \ln\frac{CO_{2,t-1}}{CO_{2,0}}\right] + \beta_2\,(1-\rho)\sum_{k=2}^{k=t}\rho^k \ln\frac{CO_{2,t-k}}{CO_{2,0}} + \varepsilon_t \\ \varepsilon_t &= \phi\varepsilon_{t-1} + \sigma z_t\ ,\ \{z_t\}\ IIDN\,(0,1) \\ & \quad T_0 \text{ given, } CO_{2,t} \text{ concentration of } CO_2 \text{ at } t,\ CO_{2,0} \text{ preindustrial concentration,} \end{aligned}$$

to regional yearly temperature data generated by their AOGCM for one scenario to "train" their emulator. They then use their estimated equation for that scenario to mimic the output of their AOGCM for another scenario. They do this procedure for 47 regions. (See Castruccio et al. (2014, Table S1 in Supporting online material) for estimates.) Their performance measure suggests that the emulator does a fairly good job of mimicking the output of the much more complicated AOGCM. Castruccio et al. (2014, Figure 6) displays the emulated temperatures with the top of the display corresponding

to northern latitude regions and the bottom of the display corresponding to southern latitude regions. The pattern of higher temperatures as one moves towards the northern regions is clear.

The advantage of emulation rather than our use of the Matthews et al. (2009) and Leduc et al. (2016) approximate relationship between cumulative emissions and temperature change is that climate scientists argue that it is more appropriate to longer time scales than yearly ones, whereas yearly time scales are more appropriate for economic analysis. Brock and Xepapadeas (2017a) exhibited a plot at time scales which are appropriate for economic analysis, using MacDougall and Friedlingstein's (2015) equations that lie behind the Matthews et al. (2009) approximation of temperature response to cumulative emissions. While their plot was approximately linear at the yearly time scale, which supports using the Matthews et al. (2009) approximation at the yearly time scale, future research should use better approximations of temperature response to cumulative emissions at the yearly time scale. Future research should use the work on emulators to get a better model of climate dynamics in our model.

References

[1] Alexeev, V.A. and C.H. Jackson (2012), "Polar amplification: Is atmospheric heat transport important?" *Climate Dynamics*, DOI 10.1007/s00382-012-1601-z.

[2] Alexeev, V.A., P.L. Langen and J.R. Bates (2005), "Polar amplification of surface warming on an aquaplanet in 'ghost forcing' experiments without sea ice feedbacks," *Climate Dynamics*, DOI 10.1007/s00382-005-0018-3.

[3] Basar, T. (1989), "Time consistency and robustness of equilibria in noncooperative dynamic games," in van der Ploeg, F. and A. de Zeeuw (Eds.), *Dynamic Policy Games in Economics*, Amsteram: North-Holland, 9-54.

[4] Başar, T. and G.J. Olsder (1995), *Dynamic Noncooperative Game Theory*, London: Academic Press.

[5] Bekryaev, R., I. Polyakov and V. Alexeev (2010), "Role of polar amplification in long-term surface air temperature variations and modern arctic warming," *Journal of Climate*, 23, 3888-3906.

[6] Brock, W., G. Engström and A. Xepapadeas (2014a), "Energy balance climate models, damage reservoirs, and the time profile of climate change policy," in Bernard, L. and W. Semmler (Eds.), *The Oxford Handbook of the Macroeconomics of Global Warming*, Oxford: Oxford University Press, chapter 3.

[7] Brock, W., G. Engström and A. Xepapadeas (2014b), "Spatial climate-economic models in the design of optimal climate: Policies across locations," *European Economic Review*, 69, 78-103.

[8] Brock, W. and L.P. Hansen (2017), "Wrestling with uncertainty in climate economic models," Mimeo, Available at http://larspeterhansen.org/wp-content/uploads/2017/07/brockhansen-1.pdf.

[9] Brock, W. and A. Xepapadeas (2017a), "Climate change policy under polar amplification," *European Economic Review*, 94, 263-282.

[10] Brock, W. and A. Xepapadeas (2017b), "Spatial heat transport, polar amplification and climate change policy," in Chichilnisky, G. and A. Rezai (Eds.), *Handbook of Climate Change*, Oxford: Oxford University Press, forthcoming.

[11] Cai, Y., W. Brock and A. Xepapadeas (2017), "Climate change economics and heat transport across the globe: Spatial-DSICE," Paper presented at the ASSA Annual Meeting in Chicago, January 6-8, 2017, Available at http://purl.umn.edu/251833.

[12] Castruccio, S., D.J. McInerney, M.L. Stein, F. Crouch, R.L. Jacob and E. Moyer (2014), "Statistical emulation of climate model projections based on precomputed GCM Runs," *Journal of Climate*, 27, 1829-1844.

[13] Dietz, S. and N. Stern (2015), "Endogenous growth, convexity of damage and climate risk: How Nordhaus' framework supports deep cuts in carbon emissions," *The Economic Journal,* 125(583), 547-620.

[14] Dockner, E.J. and N.V. Long (1993), "International pollution control: Cooperative versus noncooperative strategies," *Journal of Environmental Economics and Management,* 24, 13-29.

[15] Fountain, H. (2017), "Alaska's permafrost is thawing," *New York Times*, August 23, 2017, Available at https://www.nytimes.com/interactive/2017/08/23/climate/alaska-permafrost-thawing.html.

[16] Francis, J. (2017), "Why are Arctic linkages to extreme weather still up in the air?" *Bulletin of the American Meteorological Society,* DOI: 10.1175/BAMS-D-17-0006.1.

[17] Francis, J. and N. Skific (2015), "Evidence linking rapid Arctic warming to mid-latitude weather patterns," *Philosophical Transactions of the Royal Society A*, 373, dx.doi.org/10.1098/rsta.2014.0170.

[18] Francis, J. and S. Vavrus (2014), "Evidence for a wavier jet stream in response to rapid Arctic warming," *Environmental Research Letters*, 10, 1-12.

[19] Gasparrini, A., Y. Guo, M. Hashizume, E. Lavigne, A. Zanobetti, J. Schwartz, A. Tobias, S. Tong, J. Rocklöv, B. Forsberg, M. Leone, M. De Sario, M.L. Bell, Y.-L. Leon Guo, C.-F. Wu, H. Kan, S.-M. Yi, M. de Sousa Zanotti Stagliorio Coelho, P.H. Nascimento Saldiva, Y. Honda, H. Kim and B. Armstrong (2015), "Mortality risk attributable to high and low ambient temperature: A multicountry observational study," *The Lancet*, 386, 369-375.

[20] Hassler, J., P. Krusell and A.A. Smith (2016), "Environmental macroeconomics," in Taylor, J.B. and H. Uhlig (Eds.), *Handbook of Macroeconomics*, Volume 2B, Chapter 24, Elsevier.

[21] Hsiang, S., R. Kopp, A. Jina, J. Rising, M. Delgado, S. Mohan, D.J. Rasmussen, R. Muir-Wood, P. Wilson, M. Oppenheimer, K. Larsen and T. Houser (2017), "Estimating economic damage from climate change in the United States," *Science*, 356, 1362-1369.

[22] IPCC (2013), *Climate Change 2013: The Physical Science Basis*, Contribution of Working Group I to the Fifth Assessment Report of the Intergovernmental Panel on Climate Change, Stocker, T.F., D. Qin, G.-K. Plattner, M. Tignor, S.K. Allen, J. Boschung, A. Nauels, Y. Xia, V. Bex and P.M. Midgley (Eds.), Cambridge, UK and New York, NY: Cambridge University Press.

[23] Knutti, R. (2013), "The relationship between global emissions and global temperature rise," Available at https://unfccc.int/files/science/workstreams/the_2013-2015_review/application/pdf/7_knutti.reto.3sed2.pdf

[24] Langen P.L. and V.A. Alexeev (2007), "Polar amplification as a preferred response in an idealized aquaplanet GCM," *Climate Dynamics*, 29, 305-317.

[25] Leduc, M., H.D. Matthews and R. de Elía (2016), "Regional estimates of the transient climate response to cumulative CO_2 emissions," *Nature Climate Change*, 6, 474-478.

[26] Lenton, T., H. Held, E. Kriegler, J. Hall, W. Lucht, S. Rahmstorf and H.J. Schellnhuber (2008), "Tipping elements in the Earth's climate system," *PNAS* 105(6), 1786-1793.

[27] MacDougall, A.H. (2016), "The transient response to cumulative CO_2 emissions: A review," *Current Climate Change Reports*, 2, 39-47.

[28] MacDougal, A.H. and P. Friedlingstein (2015), "The origin and limits of the near proportionality between climate warming and cumulative CO2 emissions," *Journal of Climate*, 28, 4217-4230.

[29] MacDougall, A.H., N.C. Swart and R. Knutti (2017), "The uncertainty in the transient climate response to cumulative CO_2 emissions arising from the uncertainty in physical climate parameters," *American Meteorological Society*, DOI:10.1175/JCLI-D-16-0205.1.

[30] Matthews, H.D., N.P. Gillett, P.A. Stott and K. Zickfield (2009), "The proportionality of global warming to cumulative carbon emissions," *Nature*, 459, 829-833.

[31] Matthews, H.D., S. Solomon and R. Pierrehumbert (2012), "Cumulative carbon as a policy framework for achieving climate stabilization," *Philosophical Transactions A: Mathematical, Physical and Engineering Sciences*, 370(1974), 4365-4379.

[32] Nerem, R., B. Beckley, J. Fasullo, B. Hamlington, D. Masters and G.T. Mitchum (2018), "Climate-change–driven accelerated sea-level rise detected in the altimeter era," *PNAS,* doi.org/10.1073/pnas.1717312115.

[33] Nordhaus, W. and P. Sztorc (2013), *DICE 2013-R: Introduction and User's Manual*, Yale University Technical report.

[34] North, G.R. (1975a), "Analytical solution to a simple climate model with diffusive heat transport," *Journal of the Atmospheric Sciences*, 32, 1301-1307.

[35] North, G.R. (1975b), "Theory of energy-balance climate models," *Journal of the Atmospheric Sciences*, 32, 2033-2043.

[36] North, G.R., R.F. Cahalan and J.A. Coakely (1981), "Energy balance climate models," *Reviews of Geophysics and Space Physics*, 19(1), 91-121.

[37] Pierrehumbert, R.T. (2014), "Short-lived climate pollution," *Annual Review of Earth and Planetary Science*, 42, 341-379.

[38] Rowat, C. (2007), "Non-linear strategies in a linear quadratic differential game," *Journal of Economic Dynamics and Control*, 31, 3179-3202.

[39] Schuur, E.A.G., A.D. McGuire, C. Schädel, G. Grosse, J.W. Harden, D.J. Hayes, G. Hugelius, C.D. Koven, P. Kuhry, D.M. Lawrence, S.M. Natali, D. Olefeldt, V.E. Romanovsky, K. Schaefer, M.R. Turetsky, C.C. Treat and J.E. Vonk (2015), "Climate change and the permafrost carbon feedback," *Nature*, 520, 171-179.

[40] Tokarska, K.B., N.P. Gillett, A.J. Weaver, V.K. Arora and M. Eby (2016), "The climate response to five trillion tonnes of carbon," *Nature Climate Change,* 6, 851-855.

[41] van der Ploeg, F. and A. Rezai (2016), "Cumulative emissions, unburnable fossil fuel, and the optimal carbon tax," *Technological Forecasting and Social Change*, 116, 216-222.

[42] Whiteman, G., C. Hope and P. Wadhams (2013), "Climate science: Vast costs of Arctic change," *Nature*, 499, 401-403.

[43] Wu, W. and G.R. North (2007), "Thermal decay modes of a 2-D energy balance climate model," *Tellus A*, 59(5), 618-626.